

We are IntechOpen, the world's leading publisher of Open Access books Built by scientists, for scientists

4,800

Open access books available

122,000

International authors and editors

135M

Downloads

Our authors are among the

154

Countries delivered to

TOP 1%

most cited scientists

12.2%

Contributors from top 500 universities



WEB OF SCIENCE™

Selection of our books indexed in the Book Citation Index
in Web of Science™ Core Collection (BKCI)

Interested in publishing with us?
Contact book.department@intechopen.com

Numbers displayed above are based on latest data collected.

For more information visit www.intechopen.com



Mass Transfer Performance of a Water-Sparged Aerocyclone Reactor and Its Application in Wastewater Treatment

Xuejun Quan, Qinghua Zhao, Jinxin Xiang,
Zhiliang Cheng and Fuping Wang
*College of Chemistry and Chemical Engineering
Chongqing University of Technology, Chongqing
P.R. China*

1. Introduction

Ammonia is one of the most important contaminants impairing the quality of water resource. Ammonia is commonly present in municipal and industrial wastewater, such as landfill leachate, coke plant wastewater, and petrochemical and metallurgical wastewater. The accumulation of ammonia in water results in eutrophication and the depletion of oxygen due to nitrification (Tan et al., 2006). Moreover, wastewaters containing ammonia are often toxic, which makes their biological treatment unfeasible (Hung et al., 2003). Such adverse effects of ammonia promote the development of various techniques for its removal for instance, biological nitrification-denitrification (Calli et al., 2005; Dempsey et al., 2005), air stripping (Bonmati & Floatats, 2003; Basakcildan-kabakci et al., 2007; Marttinen et al., 2002; Ozturk et al., 2003; Saracco & Genon, 1994), struvite precipitation (Jeong & Hwang, 2005; Lee et al., 2003; Uludag-Demirer et al., 2005; Rensburg et al., 2003), membrane separation (Tan et al., 2006), catalytic liquid-phase oxidation (Huang et al., 2003), and selective ion exchange (Jorgensen & Weatherley, 2003).

The air stripping process with relatively low cost and simple equipment is widely used in the removal of ammonia from wastewater, and high rates of ammonia removal can be achieved (Ozturk et al., 2003). In addition to this process, other processes like absorption can recover ammonia that is transferred from the liquid phase to the air stream (Bonmati & Floatats, 2003). Therefore, air stripping is a good method for the removal and recovery of valuable ammonia from wastewater. In order to get high process efficiency, air stripping is usually operated in a packed tower because it can provide a larger mass transfer area (Djebbar & Naraitz, 1998). However, in practice, air stripping in packed towers usually leads to scaling and fouling on packing because of reactions between CO_2 in air and some metal ions in wastewater. In order to reduce cost, slaked lime is usually used to adjust the pH value of wastewater, thus forming a suspension. But a packed tower is not suitable for the air stripping of this kind of suspension because of the presence of solid particles that are seen in the suspension. Additionally, air stripping is a time consuming process when using some traditional equipments, because of a lower mass transfer coefficient of ammonia from the liquid to gas phase.

In recent years, some new gas-liquid contactors, with high mass transfer rate but without packing, have been used for the gas-liquid operation (Bokotko et al., 2005). Because

ammonia is a soluble gas with a small Henry's law constant, the overall mass transfer resistance in the air stripping largely lies on the gas film side (Matter-Muller et al., 1981). Therefore, decreasing the gas film resistance and increasing the gas-liquid contact area will accelerate the mass transfer of ammonia from the liquid to gas phase. A newly designed gas-liquid contactor, water-sparged aerocyclone (WSA), was developed in this work. The WSA is suitable for the air stripping of wastewater with suspended solids and has a higher mass transfer rate than some traditional stripping equipment like packed towers and tanks.

The overall mass transfer performance of the WSA was investigated using the air stripping of ammonia from wastewater. Further, in order to reveal the mass transfer mechanism of this new mass transfer equipment, the effects of major parameters on the pressure drop of gas phase, liquid side mass transfer coefficient k_L and specific mass transfer area a were also investigated. As a new gas-liquid mass transfer equipment, the WSA was used to simultaneously remove $\text{NH}_3\text{-N}$, total P and COD from anaerobically digested piggery wastewater using cheap $\text{Ca}(\text{OH})_2$ as the precipitant for PO_4^{3-} and some organic acids, and as pH adjuster for $\text{NH}_3\text{-N}$ stripping.

2. Experimental setup and methods

2.1 Design of the WSA reactor

The WSA reactor is essential equipment for the air stripping of ammonia from water; its configuration is shown in Fig. 1. In operation, the wastewater containing ammonia is pumped into the water jacket and then sparged towards the centerline of the WSA through the porous section of the inner tube wall, thus forming a large gas-liquid contact area. The transfer of ammonia from liquid to air is high because of the very small amount of liquid.

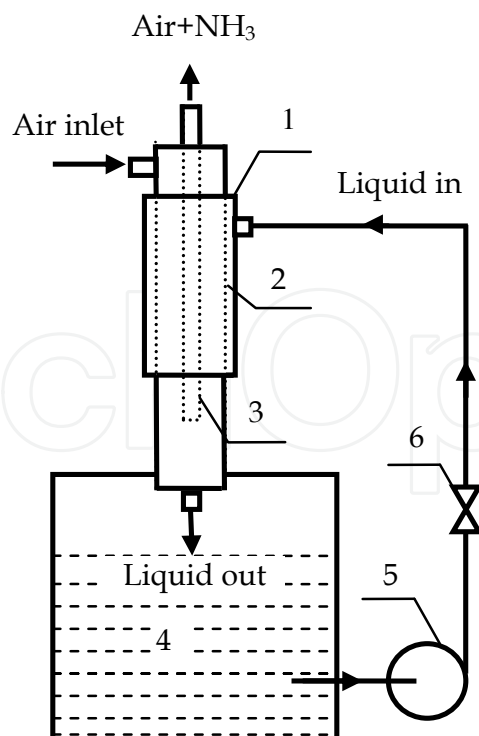


Fig. 1. The water-sparged aerocyclone reactor (WSA). 1-outer tube; 2-porous section of inner tube; 3-central gas tube; 4-water tank; 5-circulating pump; 6-valve.

The WSA reactor unit consists of two concentric right-vertical tubes and a conventional cyclone header at the top. The inner diameter of the inner tube is 0.09 m, which uses the upper section design as a porous structure for the jetting of water. 160 small holes with a diameter of 2 mm are arranged in axial symmetry on the porous section (8 holes per circle and 20 circles with an interval of 10 mm along each axial direction). The outer tube secures even distribution of water through the porous tube. The length of the porous tube section is 0.3 m and the overall length of the inner tube is 0.6 m. Wastewater is supplied through the porous section of the inner tube, and sprayed towards the centerline of the WSA. Compressed air is tangentially fed into the aerocyclone at the top header of the inner tube. Ammonia containing water is kept in the 100 l water tank, and circulated by a centrifugal pump. The water in the tank is heated by an electric heating element when needed, and its temperature is controlled by a thermocouple and measured accurately with a temperature meter. The pressure drop in the WSA is measured with a manometer. The valves located on the pipelines to the aerocyclone are used for the control of the gas and liquid phase flow rates.

2.2 Experimental setup design

The air stripping of ammonia from water is carried out in a specially designed system shown in Fig. 2.

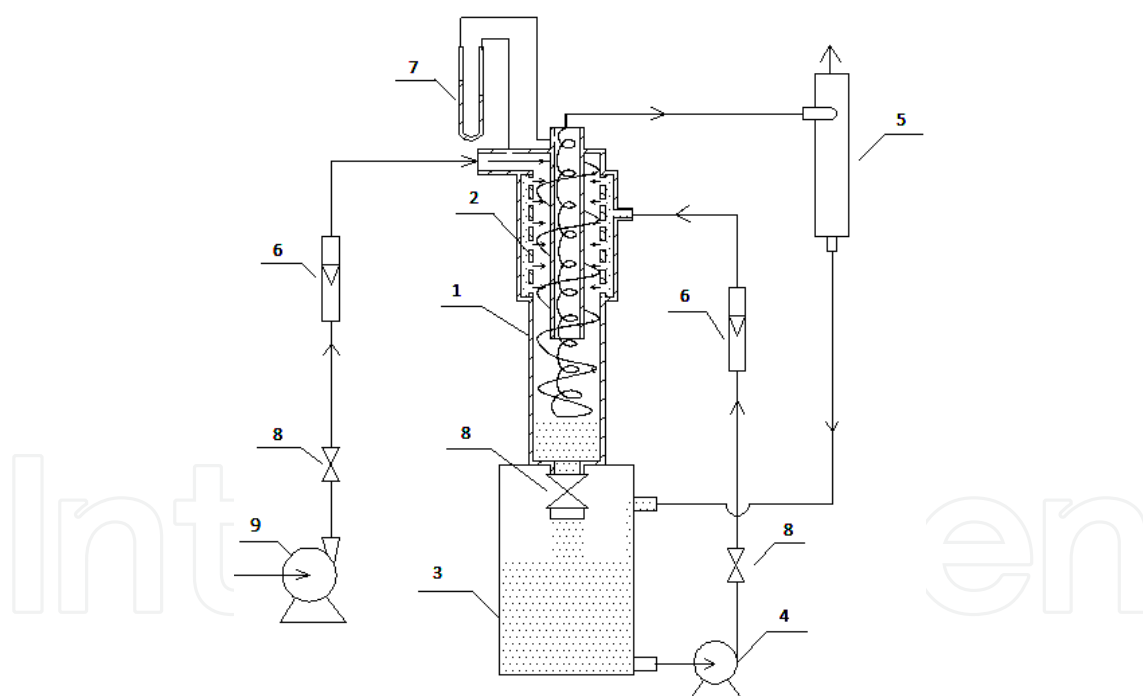


Fig. 2. The flow diagram of the experimental setup and the WSA configuration. 1- water-sparged aerocyclone; 2- porous section; 3- water tank; 4- circulating pump; 5- gas-liquid separator; 6- rotameters; 7-U type manometers; 8- valves; 9- air pump.

The primary unit is the WSA reactor, in which the separation of ammonia from water occurs. Compressed air is produced by an air compressor and tangentially introduced into the top header of the WSA, forming a strong rotating air flow field within it. Ammonia containing water is kept in a water tank, and pumped into the water jacket between the two

concentric tubes of the WSA by a circulating pump, and finally sprayed into the airflow field. Waste gas exits out through the center gas tube in the WSA and tangentially enters the gas-liquid separator, in which liquid droplets taken out by the waste gas are separated and flow back into the water tank. Volumetric flow rates are measured by means of rotameters, whereas manometers measured the pressure. Volumetric flow rates of air and water entering the WSA is adjusted by the means of valves. The cyclone header is a part of the inner tube and has a height of 0.02 m over the porous inner tube. A rectangular gas inlet gap with 0.003 m width and 0.02 m length is tangentially connected with the cyclone header. The gas flow rate was controlled within 1.1~1.9 l/s, which was an equivalent of the gas inlet velocity of 18.3 ~ 31.7 m/s.

2.3 Experimental procedure

In all the experiments, 10 l fresh aqueous $\text{Ca}(\text{OH})_2$ suspensions with different ammonia concentrations were prepared just before the experiment. Primary experiments indicate that a $\text{Ca}(\text{OH})_2$ dosage of 4 g/l can be used for maintaining a constant pH value of the suspension, which is always 11~12; and lower than 2 g/l of dosage can not maintain a constant pH value, causing an unsteady air stripping process. The ammonia equilibrium in the aqueous solution is pH and temperature dependent, and the ratio of free ammonia to total ammonia can be calculated out (Bonmati & Floatats, 2003). When the pH value is 11~12, the ammonium nitrogen is almost all converted into molecular ammonia in an aqueous solution, ensuring the air stripping of ammonia. Under this condition, the overall performance of the WSA reactor is dependent on the mass transfer rate of ammonia from water to air.

The experiments were carried out in a batch mode. Each experiment was repeated to get experimental data with an error of less than 5 %, and the averaged value was used. Before each run, the water tank was filled with the 10 l fresh aqueous $\text{Ca}(\text{OH})_2$ suspension. Then the compressed air was allowed to enter the aerocyclone at a prescribed flow rate. When the pressure reading reached a steady state, the circulation pump at a certain flow rate pumped the suspension in the tank into the WSA. During circulation, the total ammonia concentration in the suspension is continuously decreasing and is measured at an interval. The suspension samples were taken out from the water tank and centrifuged to get a supernatant for the determination of ammonia. The ammonia concentration was measured using the Nessler's Reagent ($\text{HgCl}_2\text{-KI-KOH}$) Spectrophotometry at 420 nm according to the Standards of the People's Republic of China (GB 7479-87).

In order to understand the overall performance, the effect of major process parameters on the air stripping efficiency and mass transfer coefficient of ammonia was investigated, including the flow rate of air and suspension, initial ammonia concentration, and the temperature of the suspension. At the same time, the scaling and fouling in the WSA was observed.

2.4 The overall mass transfer coefficient of ammonia stripping in the WSA

The efficiency of ammonia removal η is defined according to the measured results, as

$$\eta = \frac{C_{in} - C_t}{C_{in}} \quad (1)$$

Where C_{in} and C_t are the ammonia concentrations in the suspension at the beginning and at any time, respectively, mg/l.

For an air stripping system, the mass transfer rate of volatile compound A from water in a batch stripping unit has been derived by Matter-Muller et al (1981) and is shown as follows:

$$-\ln \frac{c_{A_t}}{c_{A_0}} = \frac{Q_G H_A}{V_L} [1 - \exp(-\frac{K_L a V_L}{H_A Q_G})] t \quad (2)$$

where c_{A_t} and c_{A_0} are the liquid phase concentrations of compound A at any time t and at the beginning, g/m³; H_A is the dimensionless Henry's constant; K_L is the overall liquid mass transfer coefficient, m/min; a is the interface area per unit volume of liquid, m²/m³; V_L is the total volume of liquid, l; Q_G is the gas flow rate, l/min and t is the stripping time, min.

When $\frac{K_L a V_L}{H_A Q_G} \ll 1$, equation (2) becomes:

$$-\ln \frac{c_{L,At}}{c_{L,A_0}} = K_L a \cdot t \quad (3)$$

This case happens when the exit stripping gas is far from saturation.

In the present work, ammonia is an easily soluble gas and the exit stripping gas is possibly far from saturation because of the very short residence time of the stripping gas in the WSA, so the calculation of the mass transfer coefficient of ammonia removal was tentatively made according to the Eq.(3).

2.5 The determination of liquid side film mass transfer coefficient k_L and specific mass transfer area a

It is a very important work to determine the mass transfer coefficient k_L and specific mass transfer area a for the further understanding of the mass transfer characteristics of the WSA. Firstly, the determination method of specific mass transfer area has been well established using a chemical absorption of CO₂ by NaOH solution (Tsai et al., 2009). In this system, when the NaOH concentration is high enough, the reaction between CO₂ and NaOH could be seen as a rapid pseudo first order reaction with respect to CO₂, and the CO₂ concentration in the bulk solution could be regarded as zero approximately. Thus, the a could be calculated out from the following equations:

$$G_A = \beta k_L A C_i \quad (4)$$

Usually β is called chemical absorption strengthening factor; G_A is the absorption rate of CO₂, mol/s; A is the mass transfer area, m²; C_i is the concentration of CO₂ on the gas-liquid interface in equilibrium with the CO₂ fractional pressure.

According to the related chemical absorption theory and the Henry's law,

$$\beta = k'_L / k_L = \sqrt{1 + Dk_1 / k_L^2} = \sqrt{1 + \gamma^2} \quad (5)$$

$$\text{And } C_i = H p_i \quad (6)$$

And when $\gamma > 10$, $\beta \approx \gamma$, thus, from the equations 4–6, $A = \frac{G_A}{H p_i \sqrt{Dk_1}}$ and $a = A/V$, here V is

the mass transfer volume in the WSA, i.e. the whole inner volume subtracted by that of the central gas tube in the WSA.

After the specific mass transfer area was obtained, the k_L could be determined by a CO_2 – H_2O absorption system. This is a physical absorption system; the mass transfer resistance mainly lies in the liquid side film, thus,

$$G_A = k_L a V C_i \quad (7)$$

The parameters a , V , C_i could be obtained through the above-mentioned process. Thus the k_L could be calculated from Eq. 7, and $a = G_A / (k_L V C_i)$.

2.6 The determination of the pressure drop of gas phase through the WSA

The pressure drop of gas phase through the WSA, i.e. the two points between the inlet and outlet of gas phase, was determined using a U-type manometer, as shown in Fig.2, with a water-air system as working medium. In order to know the interaction of the gas-liquid phases in the WSA, the liquid content ε_L in the gas phase at the gas outlet was also determined using a gas-liquid cyclone separator.

In the experimental process, the flow rate of the liquid phase should be larger than $1 \text{ m}^3/\text{h}$, which corresponds to the jet velocity of 0.381 m/s , so as to get an even jet distribution of the liquid phase in the jet area. The experimental operation process was similar with that for the air stripping of ammonia. In order to fully understand the characteristic of hydrodynamics in the WSA, the gas phase inlet velocity was controlled within $4\text{--}20 \text{ m/s}$, wider than that in a traditional cyclone.

3. Results and discussion

As mentioned above, the objective of this work is to develop new air stripping equipment of industrial interest for the removal of volatile substances such as ammonia. Firstly, to understand the overall performance of the WSA and how the major parameters affect the performance is very important. And a comparison between the WSA and some traditional air stripping equipment should be done to assess its performance. Then the effects of major process parameters on the mass transfer coefficient in liquid side film and specific mass transfer area were carried out, so as to reveal the mass transfer mechanism in the WSA. Thirdly, the pressure drop of gas phase which can reflect the momentum transfer in the WSA was also investigated, facilitating the understanding of the mass transfer process.

3.1 The mass transfer performance of the WSA

3.1.1 Effect of initial ammonia concentration on ammonia removal efficiency

The effect of the initial ammonia concentration on the air stripping efficiency of ammonia is shown in Fig. 3. It exhibits a very high air stripping efficiency of ammonia in a wide range of ammonia concentration ($1200 \sim 5459 \text{ mg/l}$). Ammonia removal efficiency higher than 97% was achieved just with 4 h of stripping time. However, using the same volume of the suspension, achieving this efficiency of ammonia removal in a traditional stripping tank needed more than 24 h . This also illustrates that the mass transfer rate of ammonia from the suspension to air in the WSA is very high compared with some traditional stripping processes.

In order to further understand the mass transfer of ammonia in the WSA, the mass transfer coefficients under different initial ammonia concentrations could be obtained using Eq. 3, i.e. plotting $-\ln(C_i/C_{in})$ vs. stripping time t and making a linear regression between -

$\ln(C_t/C_{in})$ and stripping time t could get the mass transfer coefficients K_La shown in Fig. 3 with a very good relative coefficient ($R^2 = 0.9975 \sim 0.9991$). It clearly indicates that ammonia concentration has little effect on the mass transfer coefficients, i.e. the coefficients vary in $0.019 \sim 0.021 \text{ min}^{-1}$ even though the ammonia concentration varies greatly (from 1200 to 5459 mg/l). The reasonable explanation for this phenomenon is that the process is surely controlled by the diffusion of ammonia through a gas film.

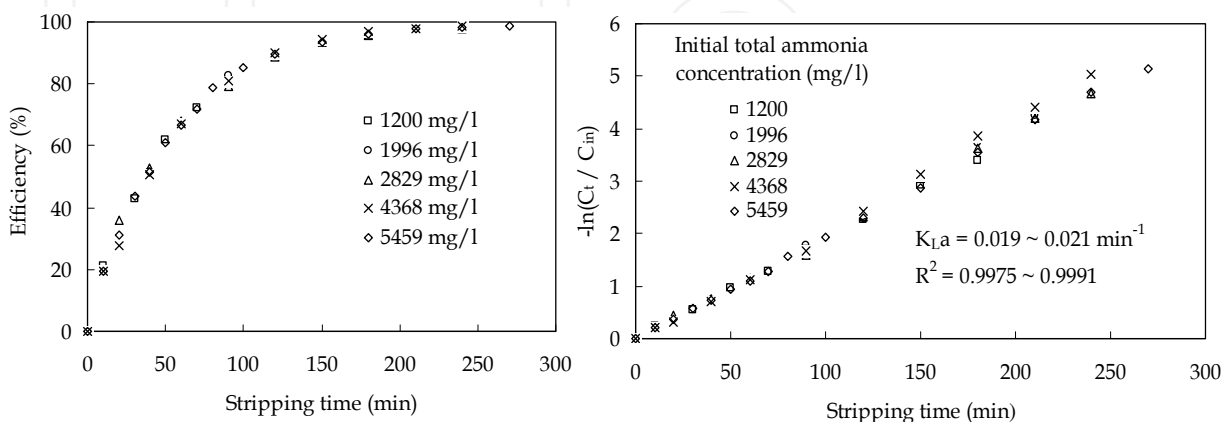


Fig. 3. Effect of initial ammonia concentration on ammonia removal efficiency (left) and mass transfer coefficients of ammonia (right) in the WSA reactor. Experimental conditions: $V_L=10 \text{ l}$, $U_L = 0.77 \text{ m/s}$, $Q_g = 1.9 \text{ l/s}$, Temperature $15 \text{ }^\circ\text{C}$, Pressure drop $0.2\text{-}0.3 \text{ MPa}$.

As shown in Fig. 3, the air stripping efficiency of ammonia is almost independent of ammonia concentration. This could be further explained according to the analysis of the mass transfer process. From Eq. 3, the following equation could be easily obtained.

$$\ln(1 - \eta) = -K_La \cdot t \quad (8)$$

Applying Eq. 8 for the air stripping process of a higher and lower concentration of ammonia suspension, respectively, $\ln(1-\eta_L) = \ln(1-\eta_H)$, i.e. $\eta_L = \eta_H$ can be obtained within a same period of stripping time because of the almost constant mass transfer coefficients K_La . That is to say, the air stripping efficiency for a system controlled by diffusion through a gas film is theoretically independent of the concentration of volatile substances. The higher the concentration, the bigger the air stripping rate. Increasing ammonia concentration can increase the driving force of mass transfer, leading to a higher rate of ammonia removal.

3.1.2 Effect of jet velocity of the aqueous phase

Increase of flow rate of the suspension may result in the increase of jet velocity of the suspension, U_L , thus changing the gas-liquid contact time and area. So, the effect of jet velocity of the aqueous phase on air stripping efficiency and mass transfer coefficient of ammonia was investigated. The results are shown in Fig. 4.

It can be seen that jet velocity of the aqueous phase has little effect on ammonia removal efficiency, and that the double increase of the jet velocity did not result in an obvious increase of the mass transfer coefficient under the experimental conditions. This illustrates that the increase of the jet velocity can not obviously increase the contact area of the two phases and can not reduce the mass transfer resistance. In the WSA, the contact area of the two phases and mass transfer resistance may be mainly determined by the gas flow rate in such a strong aerocyclone reactor, which will be investigated in subsequent section.

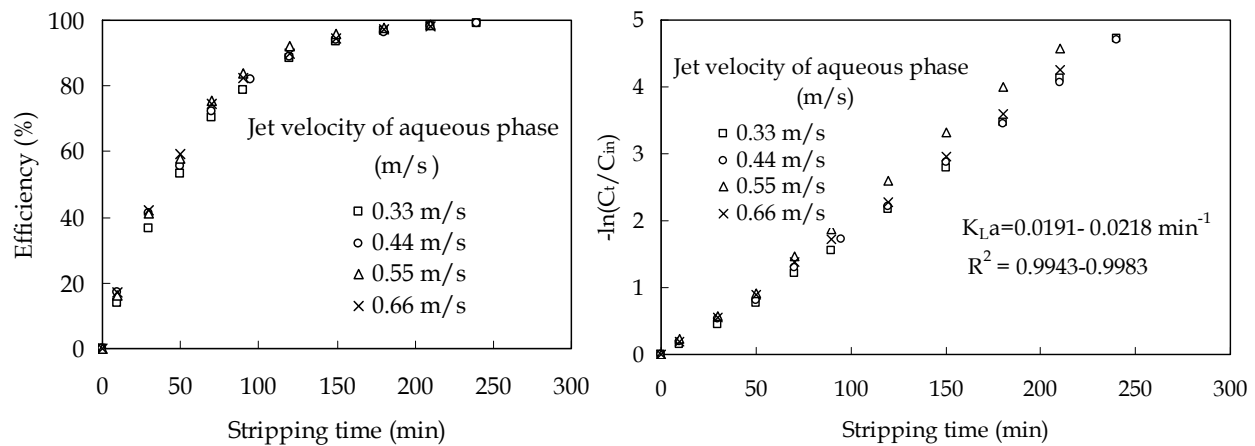


Fig. 4. Effect of jet velocity of aqueous phase on air stripping of ammonia (left) and mass transfer coefficient of ammonia removal (right). Experimental conditions: $V_L=10$ l, $Q_g=1.9$ l/s, $C_{in}=3812$ mg/l, Pressure drop 0.2-0.3 MPa, Temperature 14 - 15°C.

3.1.3 Effect of air flow rate

The effect of air flow rate Q_g on air stripping efficiency and on the volumetric mass transfer coefficient of ammonia removal is shown in Fig. 5. It seems that there is a critical value for air flow rate, which is about 1.4 l/s under the corresponding experimental conditions. When air flow rate is below this value, it has less effect on both the efficiency and the mass transfer coefficient of ammonia removal; but when air flow rate is over this value, it can result in an obvious increase in the two values.

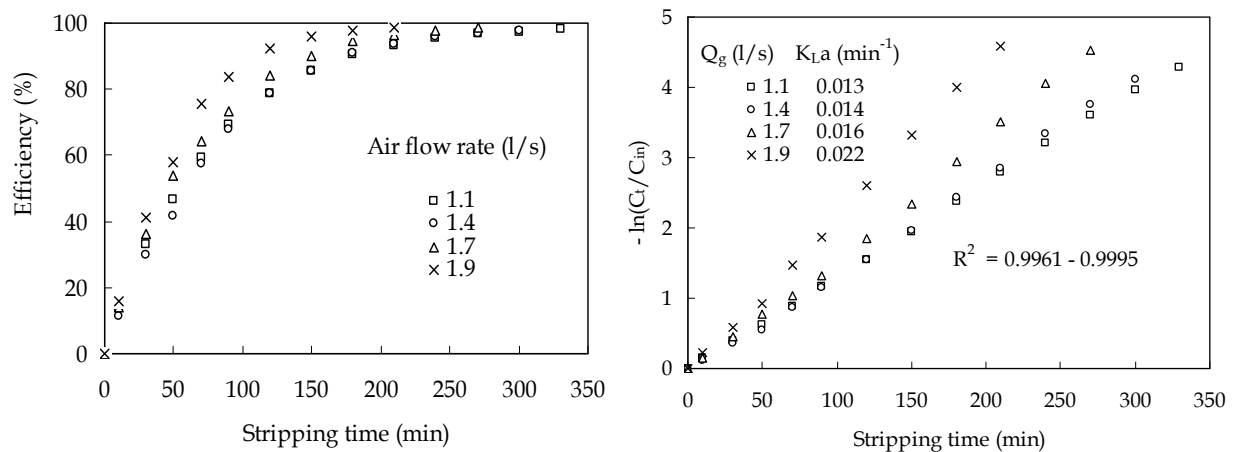


Fig. 5. Effect of air flow rate on air stripping of ammonia (left) and mass transfer coefficient of ammonia removal (right). Experimental conditions: $V_L=10$ l, $U_L=0.55$ m/s, $C_{in}=2938$ mg/l, Temperature 14 -15 °C, Pressure drop 0.12-0.3 MPa.

The phenomenon mentioned above is probably associated with the effect of the air flow on the interface of the gas-liquid phases. As mentioned above, the overall mass transfer resistance for ammonia removal is mainly present in the gas film side. The mass transfer resistance in the gas film side can be reduced by increasing the air flow rate. When the air flow rate is within a lower range (< 1.4 l/s in this work), the increase of the air flow rate has almost no effect on the mass transfer coefficient (from 0.013 to 0.014 min⁻¹) probably because

of the lower shear stress on the surface of the water droplets. Higher gas flow rate (>1.4 l/s in this work), produces larger shear stress on the droplet surface, thus clearly reducing the gas film resistance and increasing the mass transfer coefficient greatly (from 0.014 to 0.022 min^{-1}). On the other hand, a higher gas flow rate can produce larger shear stress, which exerts on the surface of the water droplets and along the porous tube surface, to cause the breakage of water drops into fine drops or even forming mist, thus leading to an obvious increase in mass transfer area. Therefore, the obvious increase in the K_{La} when the air flow rate was over 1.4 l/s may be caused by the combinational effect of this two reasons, showing clearly the effect of a highly rotating air field enhancing mass transfer between phases.

In fact, from the viewpoint of the dispersed and continuous phases, the gas-liquid mass transfer process in the WSA is similar with that in the impinging stream gas-liquid reactor (ISGLR), which enhances mass transfer using two opposite impinging streams (Wu et al., 2007). In the ISGLR, there is also a critical point of impinging velocity, 10 m/s. The effect of impinging velocity on the pressure drop increases rapidly before this critical point, and after that the effect becomes slower. The reason for this is not quite clear yet, but it is possible that a conversion of a flow pattern occurs at this point (Wu et al., 2007). Likely, the rapid increase of the mass transfer coefficient in the WSA after the critical point may be also caused by a conversion of flow patterns occurring at this point, but this needs to be further investigated. Now there are two kinds of devices that can also enhance mass transfer very efficiently, i.e. ISGLR (Wu et al., 2007) and the rotating packed bed (RPB) (Chen et al., 1999; Munjal & Dudukovic, 1989a; Munjal & Dudukovic, 1989b). Making a comparison among these devices, the WSA, ISGLR and RPB, all have essentially the same ability of enhancing the mass transfer between the gas and liquid phases. WSA and ISGLR have no moving parts, whereas RPB is rotating at a considerably high speed, and needs a higher cost and maintenance fee, and possibly has a short lifetime (Wu et al., 2007). In addition, WSA has the advantage of a simple structure, easy operation, low cost and higher mass transfer efficiency.

3.1.4 Effect of aqueous phase temperature

Both ammonia removal efficiency and the mass transfer coefficient increase with the aqueous phase temperature, as shown in Fig. 6. Particularly, when the temperature increases over 25 °C, the effect is more obvious. First, the increase of temperature will promote the molecular diffusion of ammonia in a gas film, resulting in the increase of the K_{La} . On the other hand, the gas-liquid distribution ratio K is the function of pH and temperature, and can be expressed as the following equation (Saracco & Genon, 1994):

$$K = \frac{1.441 \times 10^5 \times e^{-3513/T}}{1 + 2.528 \times 10^{-pH} \times e^{6054/T}} \quad (9)$$

Calculation indicates that when ambient temperature exceeds 25 °C, the increase of temperature will lead to a more obvious increase of the distribution ratio K . Provided the pH is high enough (such as 11), temperature strongly aids ammonia desorption from water. This makes the driving force of mass transfer increase largely. These two effects of temperature accelerate ammonia removal from water. If possible, the air stripping of ammonia should be operated at a higher temperature.

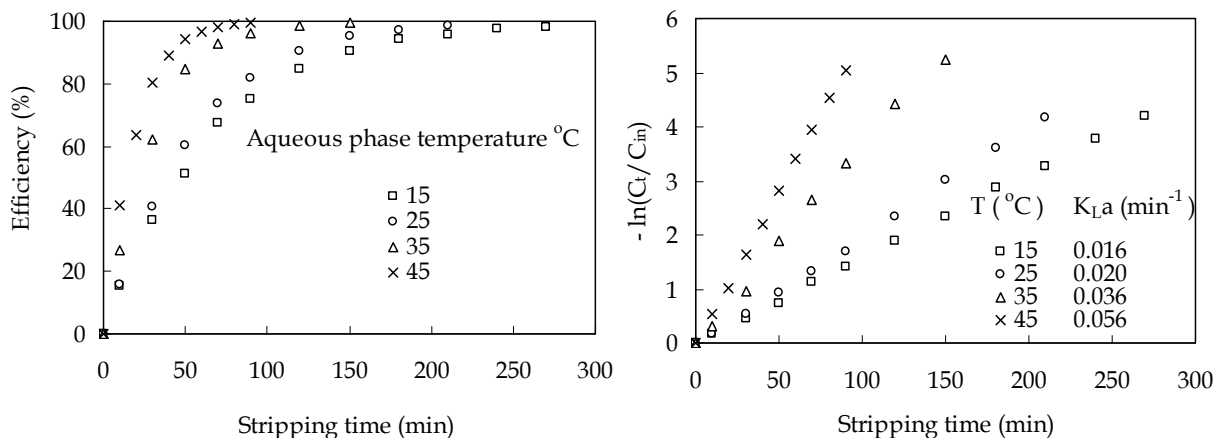


Fig. 6. Effect of aqueous phase temperature on air stripping of ammonia (left) and mass transfer coefficient of ammonia removal (right). Experimental conditions: $V_L=10$ l, $U_L=0.55$ m/s, $Q_g=1.9$ l/s, $C_{in}=2910$ mg/l, Pressure drop 0.2-0.3 MPa.

3.1.5 Comprehensive evaluation and comparison with other traditional equipments

As stated in the introduction, the main goal of the present work is to solve two problems in the air stripping of ammonia, i.e. improving process efficiency and avoiding scaling and fouling on a packing surface is usually used in packed towers. Compared with a traditionally used stirred tank and packed tower, the air stripping efficiency of ammonia in the newly developed WSA is very high because of the unique gas-liquid contact mode in the WSA. In operation of the WSA, the major parameters are air flow rate and aqueous phase temperature. In order to get a higher stripping efficiency, air stripping of ammonia should be operated at a higher air flow rate (> 1.4 l/s) and a higher ambient temperature (> 25 °C). As for scaling and fouling, after many experiments, no scale and foul were observed in the inner structure of the WSA although there were $\text{Ca}(\text{OH})_2$ particles suspended in the aqueous phase. The self cleaning effect of the WSA is probably caused by a strong turbulence of fluids in the WSA.

It is interesting to make a comparison between different air stripping processes of ammonia to understand the characteristics of the WSA. Air stripping of ammonia is generally carried out in stripping tanks and packed towers. The mass transfer coefficients of some typical stripping processes are compared in Table 1. At the same temperature, using the WSA to strip ammonia can get a higher mass transfer coefficient than using other traditional equipments; in addition, the air consumption is far less than that of the compared processes.

Equipments	Stripping conditions	Air consumption Q_G/V_L (l / l.s)	K_{La} (min^{-1})	References
WSA	$V_L = 10$ l, $Q_G = 1.9$ l/s, temperature 15 °C	0.19	0.016	This work
Tank	$V_L = 50$ ml, $Q_G = 0.08$ l/s, pH=12.0, temperature 16 °C	1.60	0.008	Basakcildan -kabakci, et al., 2007
Packed tower	$V_L= 1000$ l, $Q_G=416.7$ l/s, pH=11.0,temperature15°C	0.42	0.007	Le et al., 2006

Table 1. The comparison of the air consumption and the mass transfer coefficients of the air stripping of ammonia in different equipments.

3.2 The mass transfer mechanism within the WSA

As discussed above, air flow rate is the major parameter affecting the volumetric mass transfer coefficient $K_{L}a$ in the WSA from the viewpoint of hydrodynamics. So the effects of the gas phase inlet velocity on k_L , a and $K_{L}a$ were all further investigated using a CO_2 – NaOH rapid pseudo first order reaction system, to further elucidate the mass transfer mechanism within this new mass transfer equipment.

The results were shown in Fig. 7. It is known from Fig. 7(c) that the overall volumetric mass transfer coefficient increases almost linearly with the increasing of gas phase inlet velocity with a larger slope until the gas phase inlet velocity increases to about 10 m/s, and then almost linearly increases with a slightly lower slope, indicating that when U_g is higher than 10 m/s, the increasing rate of $K_{L}a$ with U_g was slowed down. From Fig. 7(a), it could be seen that the k_L increases very rapidly and linearly with the increase of U_g until it reaches about 8 m/s, and then the change of k_L with U_g has no remarkable behavior or even is leveled off. In contrast, the specific mass transfer area a increases proportionally with the increase of U_g almost in the whole experimental range of the gas phase inlet velocity, as shown in Fig. 7(b). Therefore, both k_L and a simultaneously contribute to the increase of the overall $K_{L}a$ before about 8 m/s of U_g making it increase rapidly; after that only a contributes to the increase of the $K_{L}a$, leading to the slowing down of its increase.

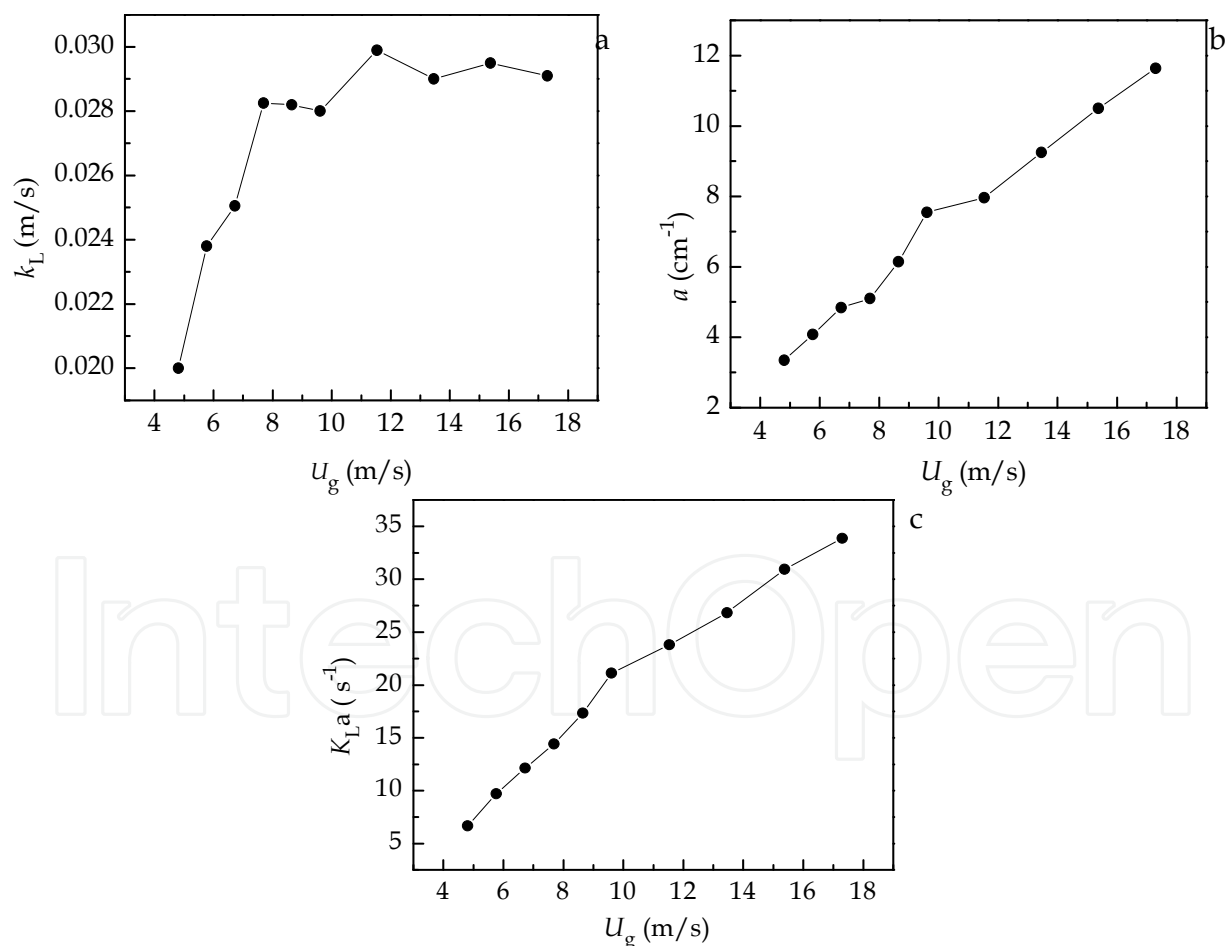


Fig. 7. Effect of gas phase velocity on the mass transfer coefficient in liquid side film (a), the specific mass transfer area (b) and the volumetric mass transfer coefficient (c) within the WSA for CO_2 – NaOH system. Experimental conditions: $U_L=0.33$ m/s, Liquid phase temperature 27~29.7 °C.

As a result, it appears that the gas cyclone field in the WSA does intensify the mass transfer process between gas-liquid phases. There is a critical gas phase inlet velocity. When U_g is lower than this value, the increase of the inlet velocity has a double function of both intensifying k_L and increasing mass transfer area; whereas when U_g is larger than this value, the major function of U_g increase is to make the water drops in the WSA broken, mainly increasing the mass transfer area of gas-liquid phases. From the viewpoint of hydrodynamics, increasing the U_g will intensify the gas cyclone field in the WSA and increase the shear stress on the water drops, thus resulting in the thinning of the gaseous boundary layer around the water drops and facilitating the increase of k_L . However, when the thinning of the boundary layer is maximized by the increase of U_g , the change of k_L will become leveled off with increasing the U_g . So theoretically, there should be a critical value, as mentioned above, which could make the k_L maximized.

3.3 The pressure drop characteristic of gas phase through the WSA

The pressure drop of gas phase ΔP and the liquid content ε_L through the WSA were simultaneous measured in this work, so as to more clearly understand the transport process occurring in the WSA. The changes of ΔP and ε_L with U_g under different water jet conditions are shown in Fig. 8.

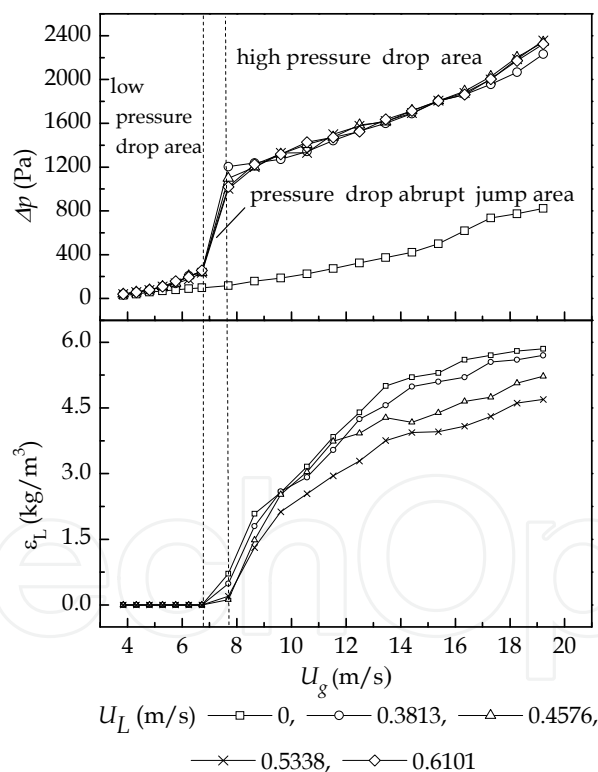


Fig. 8. Effect of inlet gas velocity on pressure drop and liquid holdup at different jet velocities.

It could be seen that when there was no liquid jet in the WSA, i.e. $U_L = 0$, the ΔP increased continuously with the increase of U_g , exhibiting the pressure drop characteristic of a traditional cyclone. Further it was observed that the data could fit the pressure drop formula, Eq.10 very well, and the resistance coefficient $\xi = 3.352$.

$$\Delta p = \xi \frac{U_g^2}{2} \rho_g \quad (10)$$

where ΔP —pressure drop, Pa; ξ —resistance coefficient; U_g — gas phase inlet velocity, m/s; ρ_g — gas phase density, kg/m³.

Meanwhile, it could be also seen that when there was jet in the WSA, the change of the ΔP with U_g was obviously different from that for a traditional cyclone. When $U_g < 6.728$ m/s, $\varepsilon_L \approx 0$, the ΔP in this area was higher than that for a traditional cyclone; when $U_g \geq 7.690$ m/s, ε_L increased rapidly with U_g , and ΔP also increased continuously with the increase of U_g but had an additional pressure drop value higher than that for a traditional cyclone under a certain U_g . Here it is worthy of noting that the gas inlet velocity for ε_L rapid increase ($U_g \geq 7.690$ m/s) is very close to that for k_L maximization (about 8 m/s, as mentioned in section 3.2). So this again indirectly indicated that this value should be the critical gas inlet velocity at which water drops and jets were broken into a large number of small droplets or fog, simultaneously increasing ε_L and a . Interestingly, it can be seen that when $U_g = 6.728 \sim 7.690$ m/s, ε_L increased rapidly from zero and the ΔP jumped from a lower to a higher pressure area, the jumped height seems to equal the additional value as just stated before. It could be believed that the pressure drop jump was caused by the transformation of liquid flow pattern when the U_g increased to a critical value. And this could be justified by the abrupt increase of ε_L at $U_g = 6.728$ m/s. Thus the pressure drop within the overall experimental range of U_g could be roughly divided into three areas, respectively called low pressure drop area, pressure drop jump area and high pressure drop area. In fact, the three pressure drop areas corresponded respectively to the observed three kinds of liquid flow pattern, here respectively called steady-state jet ($U_g < 6.728$ m/s), deformed spiral jet ($U_g = 6.728 \sim 7.690$ m/s) and atomized spiral jet ($U_g \geq 7.690$ m/s).

Further it could be seen from Fig. 8 that when $U_g > 6.728$ m/s, the liquid jet velocity had little effect on the ΔP , thus indicating the dominant role of the gaseous cyclone field in the WSA. This is in agreement with the conclusion that the gas phase inlet velocity is the major process parameter, as stated above. From the experimental results and the related discussion mentioned above, the ΔP , $K_L a$ and ε_L all increased with the increase of U_g , this further indicated that the mass and momentum transfer processes in the WSA were closely interlinked and occurred simultaneously.

The major factors affecting the ΔP include gas density ρ_g , gas viscosity μ_g , gas inlet velocity U_g , liquid density ρ_L , liquid jet velocity U_L , the diameter of jet holes d , liquid surface tension σ_L , the inner diameter D . The following dimensionless equation could be obtained using dimensional analysis:

$$Eu_g = f(Re_g, We_L, \frac{d}{D}) \quad (11)$$

Here, $Eu_g = \frac{\Delta p}{\rho_g U_g^2}$ is the Euler number; $Re_g = \frac{\rho_g U_g d_0}{\mu_g}$ the Reynolds number of gas phase;

$We_L = \frac{\rho_L U_L^2 d}{\sigma_L}$ the Weber number of liquid phase and dimensionless diameter, d/D .

Using the experimental data to fit Eq. 11 could obtain the following equations:

1. For the low pressure area: $Eu_g = 1.3685 \times 10^{-4} Re_g^{1.2353} We_L^{0.0163}$, with $R^2=0.98$;
2. For the high pressure area: $Eu_g = 4.3131 \times 10^5 Re_g^{-1.2233} We_L^{0.0022}$, with $R^2=0.99$.

The dimensionless diameter d/D does not appear in the two equations because it was maintained at a constant value in the pressure drop experiments. But this will be further investigated in the near future to optimize the structure of the WSA. From these two equations, it could be seen that the power of the We_L number is too small to be neglected compared with other powers in the same equation, indicating that We_L has little effects on the ΔP . This is in agreement with the experimental result mentioned above that the jet velocity had little effect on the ΔP , and it was mainly controlled by gas inlet velocity. So ignoring the We_L in Eq.11 and using the experimental data to fit it again, the following equations could be obtained:

1. For the low pressure area: $Eu_g = 1.4111 \times 10^{-4} Re_g^{1.2353}$, with $R^2=0.98$;
2. For the high pressure area: $Eu_g = 4.3371 \times 10^5 Re_g^{-1.2234}$, with $R^2=0.99$.

These equations apply for $Re_g = 2.3 \times 10^3 \sim 11.7 \times 10^3$ and $We_L = 3.98 \sim 10.21$, and the relative deviation between the experimental and calculated values using the above equations, is less than 7.7 % in the whole range of experimental data, showing a satisfactory prediction, as shown in Fig. 9.

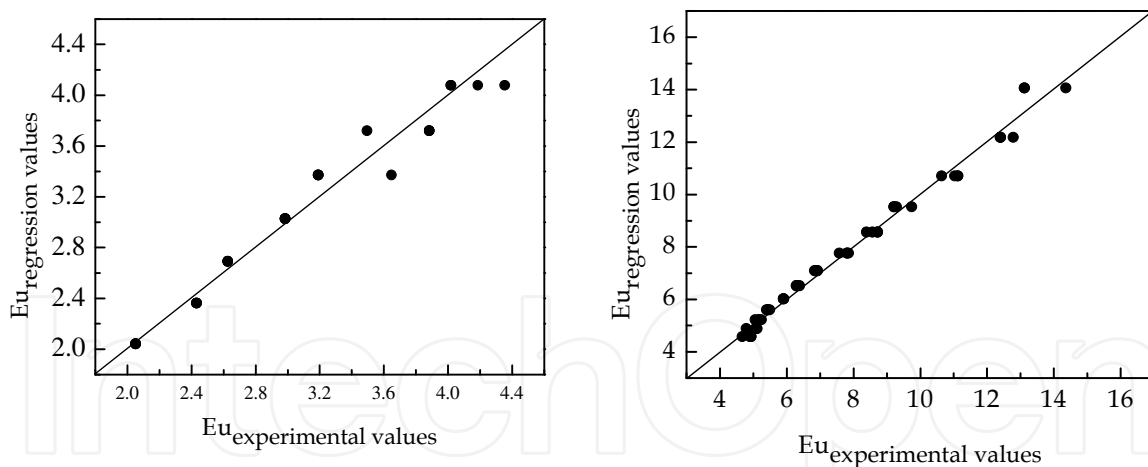


Fig. 9. Compares of regression values and experimental values, (left) low pressure drop area (right) high pressure drop area.

4. The application of the WSA in wastewater treatment

As a mixer and stripper, the WSA could be used for the precipitation of some hazardous materials and for the stripping of volatile substances in wastewaters. As an example, the WSA and the experimental setup as shown in Fig. 2, was used for the treatment of an anaerobically digested piggy wastewater (Quan et al., 2010).

Pig farms with hundreds to several thousands of animals are in operation in many countries without adequate systems for waste treatment and disposal (Nikolaeva et al., 2002). A large amount of piggery waste is discharged from the cages every day. This waste is a mixture of feces, urine and food wastage (Sanchez et al., 2001). Piggery waste is characterized by a high content of organic matter and pathogenic microorganisms. Anaerobic digestion could be considered as one of the most promising treatment alternatives for this kind of waste. In practice, many large scale pig farms in Chongqing area collect the liquid and solid fractions of piggery waste separately in pig cages to minimize the amount of piggery waste. This collection mode is a water-saving process and is beneficial to subsequent treatment. The solid fraction is directly transported to an anaerobic digester for fermentation to make organic fertilizer. The liquid fraction, a mixture of pig urine, manure leachate and washing wastewater, flows into an anaerobic digester after passing through a simple screen mesh. Practice illustrates that anaerobic digestion can greatly reduce the COD of piggery wastewater (Nikolaeva et al., 2002). Practical operation of anaerobic digestion in many pig farms in Chongqing area can make the COD of piggery wastewater to be reduced to lower than 500 mg/l. But the anaerobically digested liquor usually still contains more than 160 mg/l of $\text{NH}_3\text{-N}$ and more than 30 mg/l of total P. The national discharge standards of pollutants for livestock and poultry breeding stipulated that the COD, $\text{NH}_3\text{-N}$ and total P must be lower than 400 mg/l, 80 mg/l and 8.0 mg/l, respectively (GB 18596-2001). So the anaerobically digested liquor of piggery wastewater needs to be further treated to make its COD, especially $\text{NH}_3\text{-N}$ and total P to be decreased to lower than the required values stipulated by the national standards.

The further removal of $\text{NH}_3\text{-N}$ and total P from anaerobically digested liquor can be conducted using air stripping (Bonmati & Floatats, 2003; Basakcilar-dan-kabakci et al., 2007; Marttinen et al., 2002; Ozturk et al., 2003; Saracco & Genon, 1994) and struvite precipitation (Jeong & Hwang, 2005; Lee et al., 2003). Similar with the struvite precipitation, it was reported that calcium ions can be also used as a precipitant to form $\text{CaNH}_4\text{PO}_4\cdot 4\text{H}_2\text{O}$ (Li et al., 2007). This work presented an efficient integrated process, which consists of chemical precipitation and air stripping, for the simultaneous removal of $\text{NH}_3\text{-N}$, total P and COD from anaerobically digested piggery wastewater. In the process, cheap $\text{Ca}(\text{OH})_2$ was chosen as the precipitant for NH_4^+ and PO_4^{3-} , as pH adjuster for the air stripping of ammonia. The WSA was used to validate the large scale application possibility of the suggested simultaneous removal process.

The anaerobically digested liquor of piggery wastewater used in this experiment was taken from the effluent of the largest pig farm in Chongqing city, China. The pig farm is located in the Rongchang County, the modern animal husbandry area of China, about 100 km northwest of Chongqing city. The liquid and solid fractions of piggery waste are separately collected in the pig farm. The liquid fraction (a mixture of urine, leachate of manure and washing water) flows into an anaerobic digester after passing through a simple plastic screen. The effluent generally contains COD 150~500 mg/l, more than 160 mg/l of $\text{NH}_3\text{-N}$ and more than 30 mg/l of total P and its pH is 7.3~8.0.

The simultaneous removal of N, P and COD from the anaerobically digested liquor was conducted in the new WSA, as shown in Fig. 2. For every run, 12 l of the digested liquor was poured into the water tank in the experimental setup and then added different dosages of $\text{Ca}(\text{OH})_2$ powder under proper stirring to form a suspension with a pH higher than 11. Then

the air was pumped into the aerocyclone at a prescribed flow rate. When the pressure reading reached a steady state, the circulation pump at a certain flow rate pumped the suspension in the tank into the WSA. During circulation, the concentrations of $\text{NH}_3\text{-N}$, total P and COD in the suspension were continuously decreased because of the chemical precipitation reaction, air stripping of residual ammonia and adsorption. The suspension samples were taken out from the water tank and centrifuged to get supernatants for the determination of $\text{NH}_3\text{-N}$, total P and COD. All the experiments were carried out at ambient temperature (28~30°C). Each experiment was repeated to get experimental data with an error of less than 5 %, and the averaged value was used.

The effects of process parameters, including $\text{Ca}(\text{OH})_2$ dosage, air inlet velocity (U_g) and jet velocity of liquid phase (U_L), on the simultaneous removal of $\text{NH}_3\text{-N}$, total P and COD were investigated for the optimization of operation conditions. All the results were shown in Figs. 10-13.

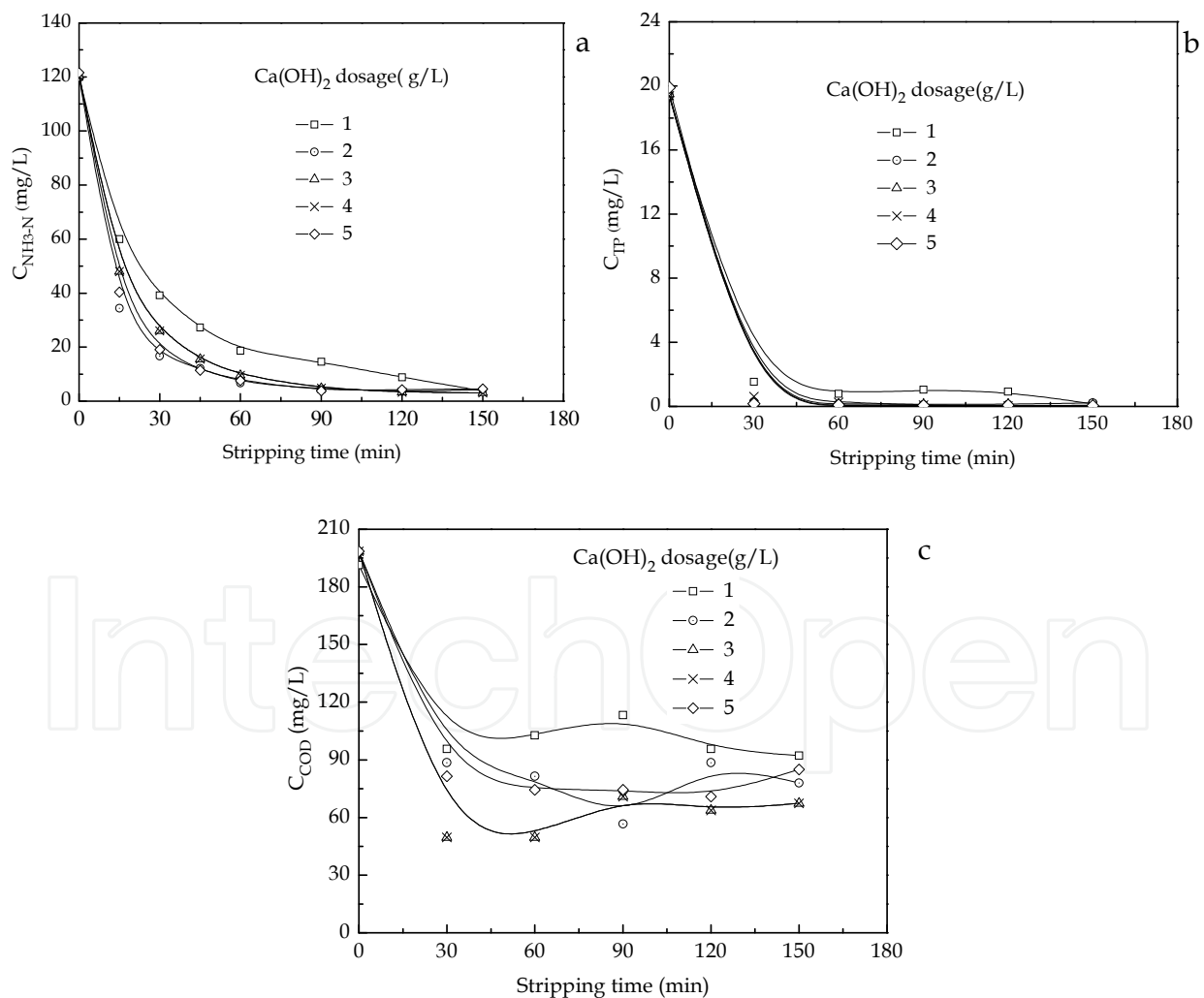


Fig. 10. The effects of $\text{Ca}(\text{OH})_2$ dosage on $\text{NH}_3\text{-N}$ (a), total P (b) and COD (c) removal. Experimental conditions: $V_L = 12$ L, $U_L = 0.37$ m/s, $U_g = 4.81$ m/s, Temperature: 28~30 °C.

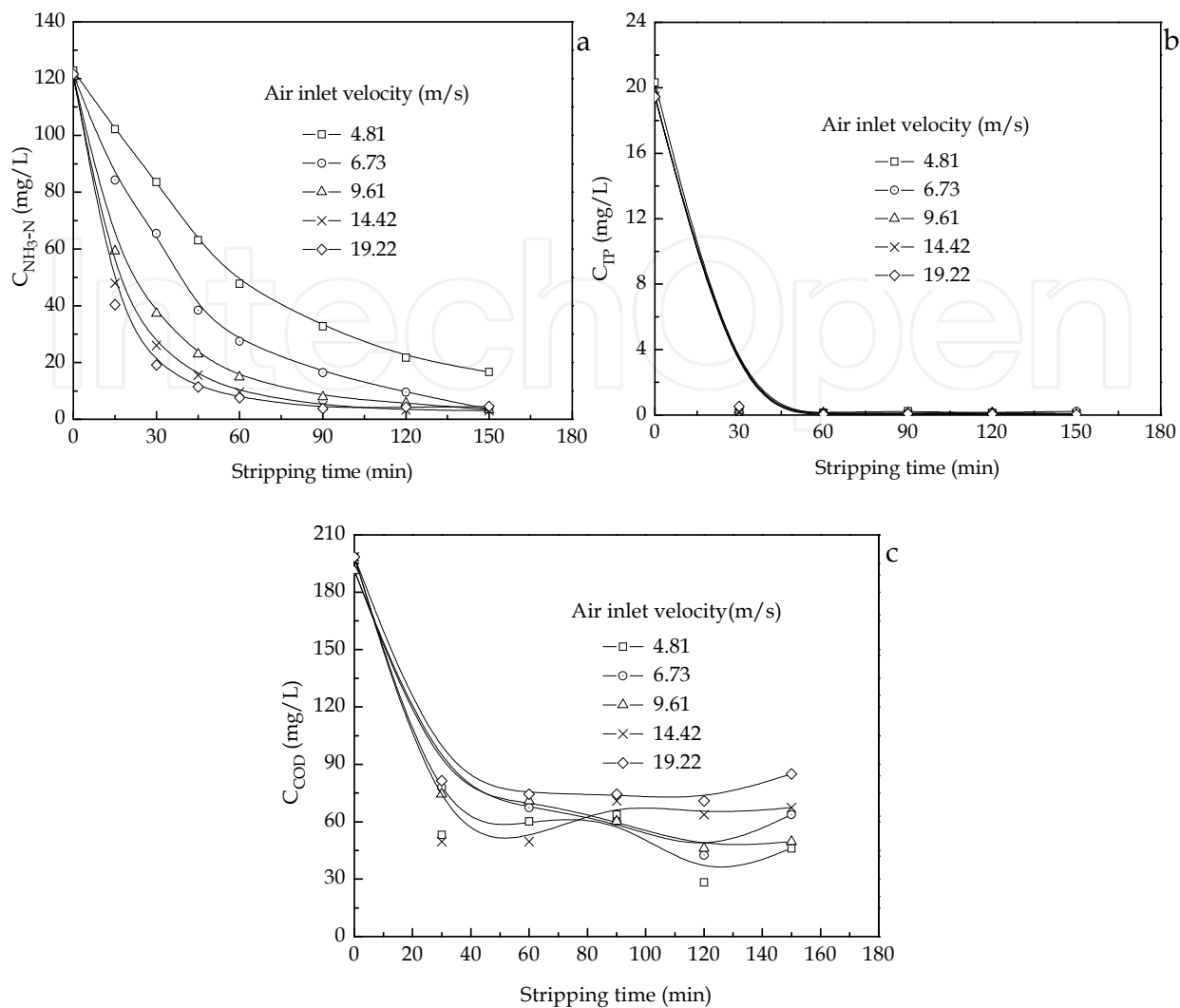
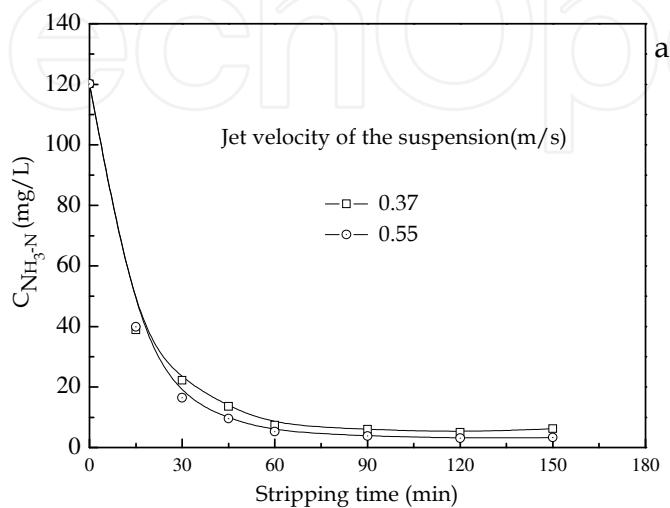


Fig. 11. The effects of air inlet velocity on NH₃-N (a), total P (b) and COD (c) removal. Experimental conditions: $V_L = 12$ L, $U_l = 0.37$ m/s, Ca(OH)_2 dosage = 3 g/l, Temperature 28~30 °C.



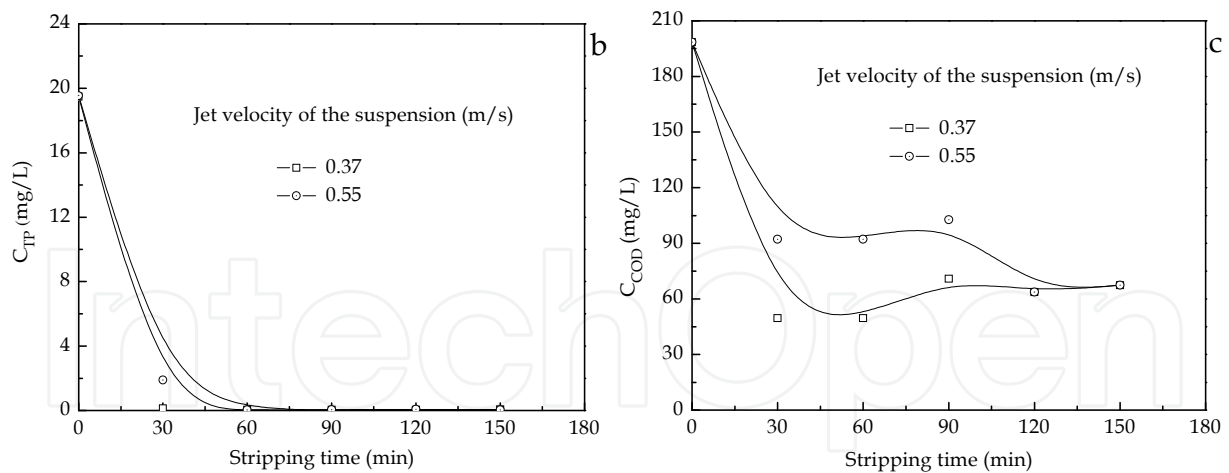


Fig. 12. The effects of jet velocity of the suspension on $\text{NH}_3\text{-N}$ (a), total P (b) and COD removal (c). Experimental conditions: $V_L = 12$ L, $U_g = 4.81$ m/s, $\text{Ca}(\text{OH})_2$ dosage = 3g/l, Temperature: 28~30 °C.

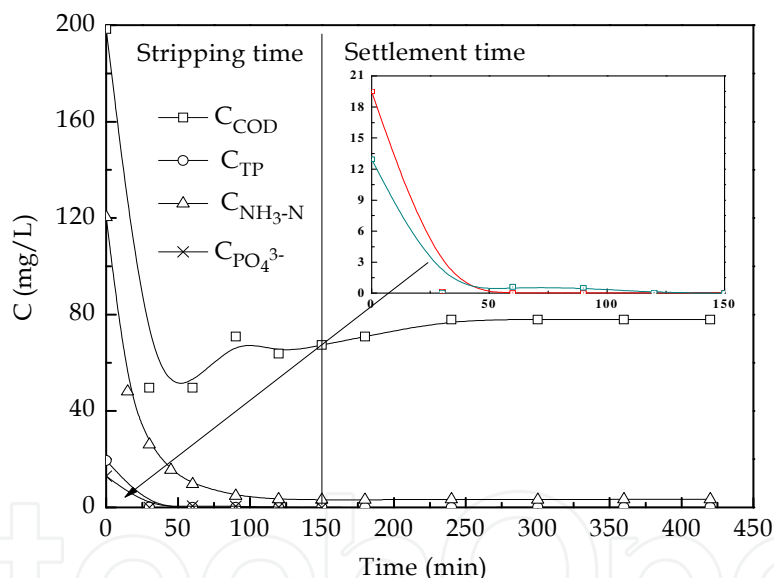


Fig. 13. The effects of stripping time and sedimentation time on $\text{NH}_3\text{-N}$, total P and COD, PO_4^{3-} removal. Experimental conditions: $V_L = 12$ L, $U_g = 4.81$ m/s, $U_l = 0.37$ m/s, $\text{Ca}(\text{OH})_2$ dosage = 3 g/l, Temperature: 28~30 °C.

It could be seen that the physicochemical process occurring in the gas-liquid-solid multiphase system in the integrated process could be conducted and operated very well in air stripping equipment without any packing. The WSA could be effectively used for the simultaneous removal of $\text{NH}_3\text{-N}$, total P and COD. 3 g/l of $\text{Ca}(\text{OH})_2$ is a proper dosage for the simultaneous removal. A higher air inlet velocity is beneficial to the removal rate of $\text{NH}_3\text{-N}$. A higher jet velocity of the liquid phase results in a faster removal of the total P. Selecting the air inlet velocity and the liquid jet velocity is needed for a better simultaneous

removal of $\text{NH}_3\text{-N}$, total P and COD. Nevertheless, in all the cases, the removal efficiencies of the $\text{NH}_3\text{-N}$, total P and COD were over 91 %, 99.2 % and 52 % for $\text{NH}_3\text{-N}$, total P and COD, respectively.

5. Conclusions

Air stripping of ammonia is a widely used process for the pretreatment of wastewater. Traditionally, this process is carried out in stripping tanks or packed towers. In practice, scaling and fouling on a packing surface in packed towers and lower stripping efficiency are the two major problems in this process.

In order to enhance process efficiency and avoid scaling and fouling in long run operations, new equipment that is suitable for air stripping of wastewater with suspended solids was developed. Air stripping of ammonia from water with $\text{Ca}(\text{OH})_2$ was performed in the newly designed gas-liquid contactor water-sparged aerocyclone (WSA). WSA exhibited a higher air stripping efficiency and an excellent mass transfer performance, and consumed less air compared with stripping tanks and packed towers. In addition, no scaling and fouling was observed in the inner structure of the WSA. The stripping efficiency and mass transfer coefficient in the WSA obviously increases with the liquid phase temperature and air flow rate. An efficient air stripping of ammonia should be conducted at a higher ambient temperature and a higher air flow rate.

In order to reveal the mechanism of the mass transfer process in the WSA, the effect of the major parameter – gas phase inlet velocity, on the liquid side film mass transfer coefficient k_L , and specific mass transfer area a was separately investigated using a $\text{CO}_2\text{-NaOH}$ rapid pseudo first order reaction system. The results indicated that there is a critical gas phase inlet velocity. When U_g is lower than this value, the increase of the inlet velocity has a double function of both intensifying k_L and increasing mass transfer area; whereas when U_g is larger than this value, the major function of U_g increase is to make the water drops in the WSA broken, increasing the mass transfer area of gas-liquid phases.

The pressure drop of gas phase ΔP was also investigated in this work, so as to more clearly understand the transport process occurring in the WSA. It was observed that when there were jets in the WSA, the change of the ΔP with U_g was obviously different from that for a traditional cyclone. And the pressure drop within the overall experimental range of U_g could be roughly divided into three areas, which could be called low pressure drop area, pressure drop jump area and high pressure drop area, respectively. In fact, the three pressure drop areas corresponded respectively to the observed three kinds of liquid flow pattern, i.e. the so called steady-state jet ($U_g < 6.728$ m/s), deformed spiral jet ($U_g = 6.728\sim 7.690$ m/s) and atomized spiral jet ($U_g \geq 7.690$ m/s). The following equations,

$$Eu_g = 1.4111 \times 10^{-4} Re_g^{1.2353} \quad \text{and} \quad Eu_g = 4.3371 \times 10^5 Re_g^{-1.2234},$$

could be used for the prediction of the gas phase pressure drop, respectively, for the low pressure area and for the high pressure area, with a satisfactory degree.

As an example, the WSA was used for the treatment of an anaerobically digested piggery wastewater. Practice showed that the WSA could be effectively used for the simultaneous removal of $\text{NH}_3\text{-N}$, total P and COD from the wastewater. 3 g/l of $\text{Ca}(\text{OH})_2$ is a proper dosage for the simultaneous removal. A higher air inlet velocity is beneficial to the removal

rate of $\text{NH}_3\text{-N}$. A higher jet velocity of the liquid phase results in a faster removal of the total P. Selecting the air inlet velocity and the liquid jet velocity is needed for a better simultaneous removal of $\text{NH}_3\text{-N}$, total P and COD. In all the cases, the removal efficiencies of the $\text{NH}_3\text{-N}$, total P and COD exceeded 91 %, 99.2 % and 52 % for $\text{NH}_3\text{-N}$, total P and COD, respectively.

6. Acknowledgements

This work was financially supported by the Chongqing Science and Technology Committee under grant no. CSTC2005AC7107, CSTC2009AB1048, and by the key discipline construction project – “Chemical Engineering and Technology” in Chongqing University of Technology.

7. References

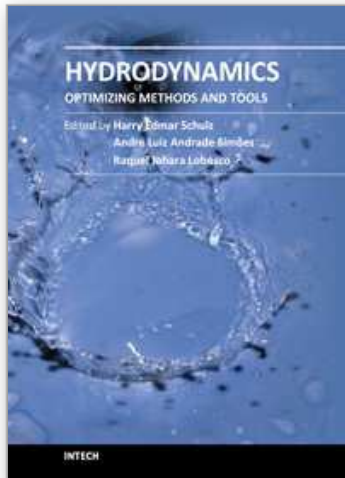
- Basakcildan-kabakci, S., Ipekoglu, A.N. & Talinli, I. (2007). Recovery of ammonia from human urine by stripping and absorption, *Environmental Engineering Science* Vol.24 (5): 615-624.
- Bokotko, R.P., Hupka, J. & Miller J.D. (2005). Flue gas treatment for SO_2 removal with air-sparged hydrocyclone technology, *Environmental Science & Technology* Vol.39: 1184-1189.
- Bonmati, A. & Floatats X. (2003). Air stripping of ammonia from pig slurry: characterization and feasibility as a pre- or post-treatment to mesophilic anaerobic digestion, *Waste Management* Vol.23: 261-272.
- Calli, B., Mertoglu, B. & Inanc, B. (2005). Landfill leachates management in Istanbul: applications and alternatives, *Chemosphere* Vol.59: 819-829.
- Chen, H., Deng, X., Zhang, J. & Zhang J. (1999). Measurements of the effective interface area and volumetric mass transfer coefficient in a multistage rotating packed bed with centrifugal atomizing by chemical adsorption, *Chemical Reaction Engineering & Processing* Vol.15 (1): 97-103 (in Chinese).
- Dempsey, M.J., Lannigan, K.C. & Minall, R.J. (2005). Particulate-biofilm, expanded-bed technology for high-rate, low-cost wastewater treatment: Nitrification, *Water Research* Vol.39: 965-974.
- Djebbar, Y. & Naraitz, R.M. (1998). Improved Onda correlations for mass transfer in packed towers, *Water Science Technology* Vol.38 (6): 295-302.
- GB 18596-2001. The national standard of the People’s Republic of China – discharge standard of pollutants for livestock and poultry breeding.
- Hung, C.M., Lou, J.C. & Lin, C.H. (2003). Removal of ammonia solutions used in catalytic wet oxidation processes, *Chemosphere* Vol.52: 989-995.
- Jeong, Y.K. & Hwang, S.J. (2005). Optimum doses of Mg and P salts for precipitating ammonia into struvite crystals in aerobic composting, *Bioresource Technology* Vol. 96: 1-6.
- Jorgensen, T.C. & Weatherley, L.R. (2003). Ammonia removal from wastewater by ion exchange in the presence of organic contaminants, *Water Research* Vol.37: 1723-1728.

- Lee, S.I., Weon, S.Y., Lee, C.W. & Koopman, B. (2003). Removal of nitrogen and phosphate from wastewater by the addition of bittern, *Chemosphere* Vol.51: 265-271.
- Le, L., Wang, H.W. & Lu, H.H. (2006). Nitrogen removal using an air stripping tower in an urban wastewater treatment plant, *China Water & Wastewater* Vol.17: 92-95 (in Chinese).
- Li, Y.F., Yi, L.X., Ma, P.C. & Zhou, L.C (2007). Industrial wastewater treatment by the combination of chemical precipitation and immobilized microorganism technologies, *Environmental Engineering Science* Vol.24: 736-744.
- Marttinen, S.K., Kettunen, R.H., Sormunen, K.M., Soimasuo, R.M. & Rintala, J.A. (2002). Screening of physical-chemical methods for removal of organic material, nitrogen and toxicity from low strength landfill leachates, *Chemosphere* Vol. 46: 851-858.
- Matter-Muller, C., Gujer, W. & Giger, W. (1981). Transfer of volatile substances from water to the atmosphere, *Water Research* Vol.15: 1271-1279.
- Munjal, S. & Dudukovic, P. (1989a). Mass transfer in rotating packed beds – I Development of gas – liquid and liquid – solid mass transfer correlations, *Chemical Engineering Science*, Vol.44 (10): 2245 – 2256.
- Munjal, S. & Dudukovic, P. (1989b). Mass transfer in rotating packed beds – II Experimental results and comparison with theory and gravity flow, *Chemical Engineering Science*, Vol.44 (10): 2257 – 2267.
- Nikolaeva, S., Sanchez, E., Borja, R., Travieso, L., Weiland, P. & Milan, Z. (2002). Treatment of piggery waste by anaerobic fixed bed reactor and zeolite bed filter in a tropical climate: a pilot scale study, *Process Biochemistry* Vol.38: 405-409.
- Ozturk, I., Altinbas, M., Koyuncu, I., Arıkan, O. & Gomec-Yangin C. (2003). Advanced physical-chemical treatment experiences on young municipal landfill leachates, *Waste Management* Vol. 23: 441-446.
- Quan, X., Ye, C., Xiong, Y., Xiang, J. & Wang, F. (2010). Simultaneous removal of ammonia, P and COD from anaerobically digested piggery wastewater using an integrated process of chemical precipitation and air stripping, *Journal of Hazardous Materials* Vol.178: 326-332.
- Rensburg, P., Musvoto, E.V., Wentzel, M.C. & Ekama G.A. (2003). Modelling multiple mineral precipitation in anaerobic digester liquor, *Water Research* Vol.37: 3087-3097.
- Sanchez, E., Borja, R., Weiland, P. & Travieso, L. (2001). Effect of substrate concentration and temperature on the anaerobic digestion of piggery waste in tropical climates, *Process Biochemistry* Vol.37: 483-489.
- Saracco, G. & Genon, G. (1994). High temperature ammonia stripping and recovery from process liquid wastes, *Journal of Hazardous Materials* Vol. 37: 191-206.
- Tan, X.Y., Tan, S.P., Teo, W.K. & Li, K. (2006). Polyvinylidene fluoride (PVDF) hollow fibre membranes for ammonia removal from water, *Journal Membrane Science* Vol.271: 59-68.
- Tsai, R.E., Seibert, A.F., Eldridge R.B. & Rochelle, G.T. (2009). Influence of viscosity and surface tension on the effective mass transfer area of structured packing, *Energy Procedia* Vol.1: 1197-1204.

- Uludag-Demirer, S., Demirer, G.N. & Chen, S. (2005). Ammonia removal from anaerobically digested dairy manure by struvite precipitation, *Process Biochemistry* Vol.40: 3667-3674.
- Wu, Y., Li, Q. & Li, F. (2007). Desulfurization in the gas-continuous impinging stream gas-liquid reactor, *Chemical Engineering Science* Vol.62: 1814-1824.

IntechOpen

IntechOpen



Hydrodynamics - Optimizing Methods and Tools

Edited by Prof. Harry Schulz

ISBN 978-953-307-712-3

Hard cover, 420 pages

Publisher InTech

Published online 26, October, 2011

Published in print edition October, 2011

The constant evolution of the calculation capacity of the modern computers implies in a permanent effort to adjust the existing numerical codes, or to create new codes following new points of view, aiming to adequately simulate fluid flows and the related transport of physical properties. Additionally, the continuous improving of laboratory devices and equipment, which allow to record and measure fluid flows with a higher degree of details, induces to elaborate specific experiments, in order to shed light in unsolved aspects of the phenomena related to these flows. This volume presents conclusions about different aspects of calculated and observed flows, discussing the tools used in the analyses. It contains eighteen chapters, organized in four sections: 1) Smoothed Spheres, 2) Models and Codes in Fluid Dynamics, 3) Complex Hydraulic Engineering Applications, 4) Hydrodynamics and Heat/Mass Transfer. The chapters present results directed to the optimization of the methods and tools of Hydrodynamics.

How to reference

In order to correctly reference this scholarly work, feel free to copy and paste the following:

Xuejun Quan, Qinghua Zhao, Jinxin Xiang, Zhiliang Cheng and Fuping Wang (2011). Mass Transfer Performance of a Water-Sparged Aerocyclone Reactor and Its Application in Wastewater Treatment, Hydrodynamics - Optimizing Methods and Tools, Prof. Harry Schulz (Ed.), ISBN: 978-953-307-712-3, InTech, Available from: <http://www.intechopen.com/books/hydrodynamics-optimizing-methods-and-tools/mass-transfer-performance-of-a-water-sparged-aerocyclone-reactor-and-its-application-in-wastewater-t>

INTECH
open science | open minds

InTech Europe

University Campus STeP Ri
Slavka Krautzeka 83/A
51000 Rijeka, Croatia
Phone: +385 (51) 770 447
Fax: +385 (51) 686 166
www.intechopen.com

InTech China

Unit 405, Office Block, Hotel Equatorial Shanghai
No.65, Yan An Road (West), Shanghai, 200040, China
中国上海市延安西路65号上海国际贵都大饭店办公楼405单元
Phone: +86-21-62489820
Fax: +86-21-62489821

© 2011 The Author(s). Licensee IntechOpen. This is an open access article distributed under the terms of the [Creative Commons Attribution 3.0 License](#), which permits unrestricted use, distribution, and reproduction in any medium, provided the original work is properly cited.

IntechOpen

IntechOpen